Quantitative femto- to attomole immunodetection of regulated secretory vesicle proteins critical to exocytosis

Jens R. Coorssen,[a,b,*] Paul S. Blank,[a] Fernando Albertorio,[a] Ludmila Bezrukov,[a] Irina Kolosova,[a] Peter S. Backlund Jr.,[a] and Joshua Zimmerberg[a,*]

[a] *Laboratory of Cellular and Molecular Biophysics, National Institute of Child Health and Human Development, National Institutes of Health, Bethesda, MD 20892-1855, USA*
[b] *Department of Physiology and Biophysics, Neuroscience Research Group, Faculty of Medicine, University of Calgary, Calgary, Alta., Canada T2N 4N1*

Received 16 January 2002

Abstract

Although immunoblotting (Western blotting) is widely used for the detection of specific proteins, it is often thought to be an inadequate technique for accurate and precise measurements of protein concentration. However, an accurate and precise technique is essential for quantitative testing of hypotheses, and thus for the analysis and understanding of proposed molecular mechanisms. The analysis of Ca^{2+}-triggered exocytosis, the ubiquitous eukaryotic process by which vesicles fuse to the plasma membrane and release their contents, requires such an unambiguous identification and a quantitative assessment of the membrane surface density of specific molecules. Newly refined immunoblotting and analysis approaches permit a quantitative analysis of the SNARE protein complement (VAMP, SNAP-25, and syntaxin) of functional secretory vesicles. The method illustrates the feasibility of the routine quantification of femtomole to attomole amounts of known proteins by immunoblotting. The results indicate that sea urchin egg secretory vesicles and synaptic vesicles have markedly similar SNARE densities. © 2002 Elsevier Science (USA). All rights reserved.

Keywords: Quantitative immunodetection; Western blotting; Secretory vesicles; SNARE proteins; Protein purity

Electrophoretic transfer of proteins from urea and SDS–PAGE gels to nitrocellulose sheets, with subsequent immunodetection of < 1 ng of protein ("Western blotting"), was first reported by Towbin et al. [1] and Burnette [2]. Optimization of the technique has focused primarily on protein transfer efficiency and on detection methods such as chemiluminescence, chemifluorescence, colorimetric products, and radiolabeling. Although Western blotting is used extensively for protein identification, absolute quantitative determinations of either the amount or the concentration of protein present have been infrequent. Quantitative detection of 0.5 ng ($\sim$20 fmol) of bovine growth hormone allowed concentrations as low as 10–15 ng/ml to be detected [3], while the detection of nanogram quantities of zyxin and c-Myc proteins allowed determinations of copy number per cell [4,5]. Routine quantitative assessment of femtomole amounts, or less, of proteins is possible using the immunoblotting and analysis protocols in the present article; no additional methods or modifications to antibodies are required. This represents over an order of magnitude improvement in quantitative detection relative to standard Western blotting protocols and several orders of magnitude improvement over immunocytochemical detection, a method suited to the characterization of relative protein distributions but not to the direct analysis of molecular mechanisms.

The molecular mechanisms of exocytosis remain the subject of intense research and speculation because exocytosis is a basic and essential process in most cell types (e.g., endocrine, exocrine, hematopoietic, immune, neural). Although numerous proteins involved in the process of exocytosis have been identified [6], the cyclic nature of the interconnected pathway makes it difficult

---

*Corresponding authors.

E-mail addresses: jcoorsse@ucalgary.ca (J.R. Coorssen), joshz@ helix.nih.gov (J. Zimmerberg).

to specify at which points given proteins function, and thus, analysis of critical molecular mechanisms remains problematic [7,8]; a block at any point in the pathway will eventually inhibit secretion. As a defining stage of exocytosis, the Ca^{2+}-triggered membrane fusion steps have been the subjects of extensive research; speculation on the molecular mechanisms involved has been a major catalyst for further experimentation. One hypothesis, arising from structural and cell biological studies of the SNARE complex [9,10] and reconstitution experiments [11], has come to dominate most research concerning the mechanism of fusion. The SNAREpin hypothesis [11] suggests that a *trans* complex of the proteins VAMP, SNAP-25, and syntaxin is the central determinant of membrane interaction and that the rapid interbilayer formation of this complex ("zippering-up") overcomes the energy barriers to fusion [6,12,13]. To test this hypothesis, it is important to be able to assay fusion (rather than the entire exocytotic pathway) and concurrently quantify the density of SNARE proteins on fully functional, native secretory vesicles [7,8,14–16].

Although ghosts and isolated vesicles prepared from most cell types rapidly lose fusion competence, requiring cytosol (and thus additional molecular steps in the pathway) to retain function, cortical vesicles (CV)[1] from unfertilized sea urchin eggs, isolated from their final fully primed and Ca^{2+}-sensitive docked state, remain fully fusion-competent for hours in the absence of soluble factors, requiring only an increased free Ca^{2+} concentration ($[Ca^+]_{free}$) to trigger rapid fusion [7,8,14]. In addition, CV size ($\sim 1\,\mu m$ diameter), purity, stage specificity, substantial yields, and the apparent presence of only one form of each of the SNARE proteins [7,8] make them ideal for coupled functional and biochemical analyses. Using this approach, we have previously shown that the formation, presence, or disruption of SNARE complexes is not essential to Ca^{2+}-triggered membrane fusion [7,8,14,15]. Rather, loss of SNARE complexes is correlated with a diminished Ca^{2+} sensitivity for fusion, suggesting modulatory and/or upstream roles for the SNAREs [7]. However, these studies may have missed transient complexes and did not address other possible roles for SNAREs, either individually or in alternate/other protein complexes. To further assess the SNAREpin hypothesis, we have sought to obtain accurate estimates of the membrane surface density of VAMP, SNAP-25, and syntaxin on fully fusion-competent CV using newly refined immunoblotting and analysis approaches. With our current level of detection, accurate, and precise quantitative determinations of SNARE copy number per CV are routine. This is the first report of such a quantitative assessment. These studies indicate that fully Ca^{2+}-sensitive and fusion-competent native sea urchin egg secretory vesicles have SNARE densities that are comparable to available estimates on synaptic vesicles.

Materials and methods

Quantitative analysis of isolated membrane proteins

Isolated hydrophobic proteins from CV were analyzed as described [2,9], with 15 modifications to enhance sensitivity and reproducibility. (1) CV stocks were counted. (2) High-purity protein standards were used. (3) Efficiency of native SNARE recovery was assessed at each stage of extraction. Extraction efficiencies, relative to CV and SNARE standards put directly into SDS sample buffer, were used as correction factors to evaluate CV SNARE recoveries. (4) To avoid acid hydrolysis of proteins, SDS sample buffer (pH 8.9) was used, and SDS protein samples were boiled for 5 min prior to PAGE [17]. (5) Myoglobin was added to each protein sample prior to SDS–PAGE to capture free radicals and saturate binding sites, thus improving transfer of low-abundance proteins; gels were also soaked in buffer containing myoglobin to increase the extent/efficiency of protein transfer to PVDF membranes [18]. (6) Recombinant protein standards and dilutions of each protein sample were analyzed in parallel by SDS–PAGE. (7) SDS–PAGE was carried out slowly at 90–100 V (4 °C) to avoid deformation of protein bands [19]. (8) Proteins were electroblotted onto 0.1-μm (pore diameter) PVDF membrane to increase protein recovery and, thus, band densities for quantitative assessment by immunoblotting; during electroblotting there were measurable losses of proteins through 0.45-μm PVDF membrane (onto 0.1- or 0.45-μm backing membrane) at loads $\geqslant 1$ fmol. (9) Membrane blocking conditions were optimized (blocking solution composition and time applied) for the proteins of interest, yielding high signal-to-background ratios even when blotting onto 0.1-μm PVDF membrane. (10) Highly selective primary antibodies were used at saturating concentrations for 15 h incubations (4 °C). (11) Alkaline phosphatase-labeled secondary antibodies and enhanced chemifluorescence (ECF) reagents (Amersham) were used to detect primary antibody using 2-h incubations (room temperature). Secondary antibody controls were carried out in every experiment. (12) ECF signals were scanned (STORM, Molecular Dynamics) at the highest sensitivity possible (700 V and 100 μm²/pixel); all blots were also assessed at 500–600 V to maximize the calibration range. The scanner itself was also routinely assessed to ensure uniformity of scan area, to ensure equal detection across every blot. (13) A highly accurate determination of peak area was implemented using a Lorentzian function with a linear background to fit digitized lane scans. (14)

Digitized data were converted to amount of protein using calibration curves, and corrected for recovery to give the total amount of a CV membrane SNARE prior to extraction; CV counts made prior to protein extraction were used to establish the average number of SNAREs/CV. (15) To evaluate potential interference, the entire analysis of SNARE standards was repeated in the presence of excess CV protein; sensitivity was invariant in the presence of excess protein.

SNARE plasmids and standards

An expression clone for the cytoplasmic domain of urchin ovary syntaxin (GenBank No. AF333035) as a GST fusion protein, in the pGEX-3X plasmid, was obtained from Dr. Gary Wessel. The full-length coding region (GenBank No. AF151536) of urchin ovary VAMP (with C-terminal 6× His tag; his-VAMP) was subcloned into the pQE60 plasmid (Qiagen). A full-length urchin ovary SNAP25 (GenBank No. AF061750) with maltose-binding protein (MBP-SNAP25) was subcloned into the pMAL-c2x plasmid (New England Biolabs); C-terminal 6× His-SNAP25 (his-SNAP25) was subcloned into pQE60.

GST fusion proteins were expressed in *Escherichia coli* strain BL21 (DE3; Stratagene), and 6× His-tagged proteins in strain M15 (Qiagen). Bacterial cultures (1–4 L) were grown to an OD_{600} of 0.6–0.8, and recombinant protein expression was induced with IPTG for 2–4 h. GST–syntaxin was purified from inclusion bodies using 8 M urea and 50 mM Tris (pH 8.0), followed by dialysis into PBS (4 °C). After centrifugation at 12,000*g* for 20 min, the supernatant was incubated (1 h, 4 °C) with GSH–Sepharose (AP Biotech) and washed with PBS, and GST–syntaxin was eluted with 50 mM Tris (pH 7.5) and 10 mM reduced glutathione. GST–syntaxin was further purified by MonoQ chromatography. Factor Xa (New England BioLabs) was used to isolate syntaxin for use in antibody production.

For use as an immunoblotting standard, GST–syntaxin was purified by preparative SDS–PAGE (8% gels run at 90 V, 4 °C), localized by Coomassie staining narrow lanes on each side of the gel, and excising the region corresponding to GST–syntaxin from the unstained gel. The protein was electroeluted at 400 mA (1 h, 4 °C), precipitated with $CHCl_3/CH_3OH$, and solubilized in 62 mM Tris (pH 6.8), and the concentration was determined using A_{280} and a molar extinction coefficient of 50,240 [20]; extracts from control gels (mocks) were blanks for the A_{280} measurements.

MBP-SNAP-25 was recovered by sonication and centrifugation; soluble proteins were bound to amylose, and MBP-SNAP25 was eluted with 10 mM maltose in 20 mM Tris (pH 7.4), 200 mM NaCl, 1 mM EDTA, and 1 mM DTT. His-SNAP-25 was isolated on Ni–NTA resin, eluted with 250 mM imidizole, 50 mM sodium phosphate (pH 8.0), and 300 mM NaCl, and dialyzed against 50 mM Tris (pH 8), 150 mM NaCl, and 10 mM DTT. Purification was by preparative SDS–PAGE (14% gels, 70 V, 4 °C, 5 h) and the concentration of electroeluted his-SNAP25 was determined using A_{280} and a molar extinction coefficient of 13,260 [20].

His-VAMP was recovered using a cycle of freeze–thawing and sonication in 50 mM sodium phosphate (pH 8.0), 300 mM NaCl, and a cocktail of protease inhibitors (Complete, EDTA-free; Roche) and centrifuged. The pellet was resuspended in sonication buffer containing 1% TX-100 and again sonicated and centrifuged. The remaining pellet was dissolved in 6.0 M guanidine, 0.1 M NaH_2PO_4, 10 mM Tris (pH 8.0), and 1% Triton X-100 and centrifuged. The supernatant was added to NTA–Ni resin (Qiagen) and rocked overnight (4 °C). The resin was washed with guanidine buffer and then with buffer containing 25 mM imidazole. His-VAMP was eluted with 250 mM imidazole, purified by preparative SDS–PAGE (20% gels, 70 V, 4 °C, overnight), and electroeluted in buffer containing 1% SDS, and the concentration was determined using A_{280} and a molar extinction coefficient of 12,600 [20].

Anti-SNARE protein antibodies

Anti-human VAMP2 antibody (HV-62), directed against the conserved region (amino acids 33–94 [21]), was a gift from Dr. J.O. Dolly; this region is 90% identical to that of urchin VAMP. An antibody to the cytoplasmic domain of rat VAMP2 gave similar results but less sensitive detection (not shown). Anti-urchin syntaxin antibody produced in rabbits was used without further purification; serum showed no GST cross-reactivity. Anti-SNAP25 antibodies produced in rabbits were affinity-purified using his-SNAP25 coupled to Affigel-15 (Bio-Rad); any residual anti-MBP antibodies were removed on a MBP column.

Preparation and treatment of sea urchin egg cortical vesicles

Sea urchins (*Strongylocentrotus purpuratus*) were maintained, CV were isolated, fusion was measured, $[Ca^{2+}]_{free}$ was assessed, and hydrophobic proteins were extracted as described [2,9]. The CV pellet was suspended in baseline intracellular-like medium (B-IM buffer; 210 mM potassium glutamate, 500 mM glycine, 10 mM NaCl, 1 mM $MgCl_2$, 0.05 mM $CaCl_2$, 1 mM EGTA, 10 mM Pipes, 2.5 mM ATP, 2 mM DTT, pH 7.4) and maintained on ice. As CV are large (∼ 1 μm diameter) and optically dense, they are easily visualized and counted using phase contrast microscopy (40×) and a standard Neubauer hemacytometer. Working samples were diluted 20-fold (5 μl of sample +95 μl B-IM) and an aliquot was placed in the hemacytometer. A brief set-

tling period facilitated counting; out-of-focus CV were identified by focusing through the volume of the chamber. CV were counted in 10 of the 25 squares of the central $1 \times 1 \times 0.1$-mm^3, 25-square cytometer grid. The average count per square was determined and used to calculate the CV density in the diluted sample. A final density, CV/ml of working sample, was calculated from the diluted sample concentration. Following counting, CV were aliquoted for fusion assays and protein isolation (0 h controls) in order to assess native fusion activity and SNARE protein complement. In some cases, isolated CV were incubated for 1–4 h at 25 °C prior to extraction of hydrophobic proteins. In all cases, CV–CV fusion was assayed [2] to ensure that fully functional vesicles were being analyzed (not shown).

Results

Determination of protein purity

Quantitative immunodetection requires standard calibration curves, the accuracy of which depends upon the purity of the protein standards. A fundamental problem in assessing purity is the limited detection range of routine assays (Coomassie or silver staining following SDS–PAGE). The amounts of protein required to detect trace contaminants often result in saturation of the standard protein signal, whereas amounts of standard protein that yield a linear signal are too low for adequate contaminant detection; the result is an under- or overestimate of protein purity. The following procedure was developed to eliminate this problem; the assessment of GST–syntaxin purity is shown as an example (Fig. 1). A series of increasing standard protein concentrations was stained with Coomassie blue following SDS–PAGE (Fig. 1A). The stained gels, together with a Transmission Step Wedge (Stouffer T2115), were scanned (AGFA Arcus II scanner) in transparency or reflectance mode. Data were imported into ImageQuant software (Molecular Dynamics), permitting integrated line scans covering the length of the gel (for a range from ∼10 to 250 kDa for syntaxin) and the full width of each lane (lane scan). The 16-bit intensity units were converted into scaled optical density (OD) units [$OD_{scaled} = -\log(Intensity/2^{16})$] and the linear scanning range was established using the Transmission Step Wedge. Peak areas for the standard proteins were determined by summing the OD above a linear background. A linear calibration of total protein vs integrated OD (peak area) was determined for non-saturating amounts of standard proteins (Fig. 1B). For larger amounts of protein, permitting detection of contaminants, the predicted OD for the standard protein was estimated by extrapolation of the linear calibration curve and used to calculate purity. The total integrated OD minus the uncorrected peak area was taken as a measure of the contaminating background. Purity was calculated as the ratio of the extrapolated peak area to the sum of the contaminating background and extrapolated peak. Purity error estimates were obtained using the 95% prediction intervals for extrapolated integrated OD values at high protein loads. This is the most conservative estimate of purity, as small contaminants may not be easily distinguished from the background. The purity ($\pm 95\%$ confidence) of the isolated syntaxin was $98 \pm 1\%$. Comparable analyses done on purified recombinant urchin VAMP and SNAP-25 yielded purities of 94 ± 1 and $99 \pm 0\%$, respectively. Purities were confirmed by mass spectrometry (not shown).

Quantification of Western blots

Calibration standards were prepared using serial dilution. Immunoblots visualized with ECF were digitized using a STORM scanner (Molecular Dynamics), and the resulting data were analyzed using ImageQuant and TableCurve2D software. In addition to full lane scans (to improve signal to background level), a 5-parameter model consisting of a Lorentzian function and a linear background was used to quantify the integrated area under the peaks corresponding to the proteins of interest (Fig. 2). The fit standard errors using a Lorentzian peak function ($Y = A/(1 + (X - B)^2/C^2)$) were routinely lower than a Gaussian peak function $y = A * \exp(-0.5 * (X - B)^2/C^2)$, and the slopes of the resulting calibrations were larger, indicating greater sensitivity. This result was not unexpected since protein bands in chromatography are known to deviate significantly from a Gaussian profile, and a wide variety of peak functions have been used to characterize chromatographic profiles [22,23]. Repeated calibrations showed that the standard deviation of the integrated peak fluorescence was linear with the square root of the mean integrated peak fluorescence. This statistical behavior is expected for a Poisson counting process, the detection of fluorescence. For this reason, weighted linear regression (1/(Integrated Peak Fluorescence)) was used in determining the limits of detection and sensitivity of calibration Western blots. The limit of detection is defined as the amount of protein corresponding to the value of the integrated peak fluorescence that is three times the standard error of the fit.

Electrotransfer through standard PVDF membrane

Proteins were initially electroblotted onto standard PVDF membrane (0.45-μm pore size) and detected by ECF rather than by chemiluminescence, as previously used [2,9]. However, placing an additional sheet of PVDF membrane (0.1- to 0.45-μm pore size) behind the first during electrotransfer captured detectable amounts of proteins that would have been lost to detection using
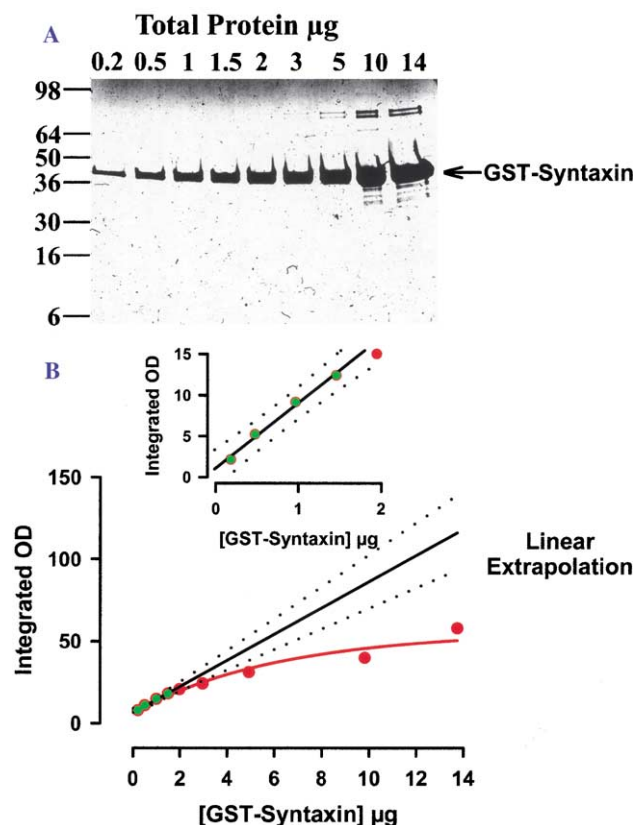
Fig. 1. Syntaxin purity. (A) Recombinant sea urchin ovary syntaxin was analyzed by SDS–PAGE, and the resulting gels were stained with Coomassie blue for determination of purity. Comparable analyses were done on isolated recombinant urchin VAMP and SNAP-25. The identity and purity of all recombinant protein standards were confirmed by MALDI mass spectrometry (Voyager DE-STR; Perspective Biosystems). (B) The gel in (A) was scanned and analyzed by densitometry (see Materials and methods). The total areas of bands corresponding to syntaxin were plotted relative to the total amounts of recombinant syntaxin originally loaded. Overloading and thereby saturating the syntaxin signal in some lanes reveal the extent of bacterial protein contamination. By linear regression, a straight line is fit through those points corresponding to nonsaturating syntaxin loads (green circles); this regression line in extrapolated to include the entire range of syntaxin loads analyzed (red circles) and used to calculate purity. The difference between the total scan area and the area of the syntaxin peak was used to quantify impurities.

standard Western blotting procedures; electrotransfer through the membrane occurred with all three proteins studied. An example of the electrotransfer of VAMP through a 0.45-µm PVDF membrane is shown in Fig. 3. While the exact relationship between protein loss and molecular weight, pore size, and transfer conditions is not well characterized, we found that detectable amounts of each of the SNAREs were routinely lost through the PVDF membrane. Electrotransfer of proteins through 0.45-µm pore-size nitrocellulose membranes is a known problem that compromises the accuracy of quantitative protein determinations [24,25]. We optimized conditions to routinely utilize the 0.1-µm PVDF in our immunoblotting procedures (see Materials
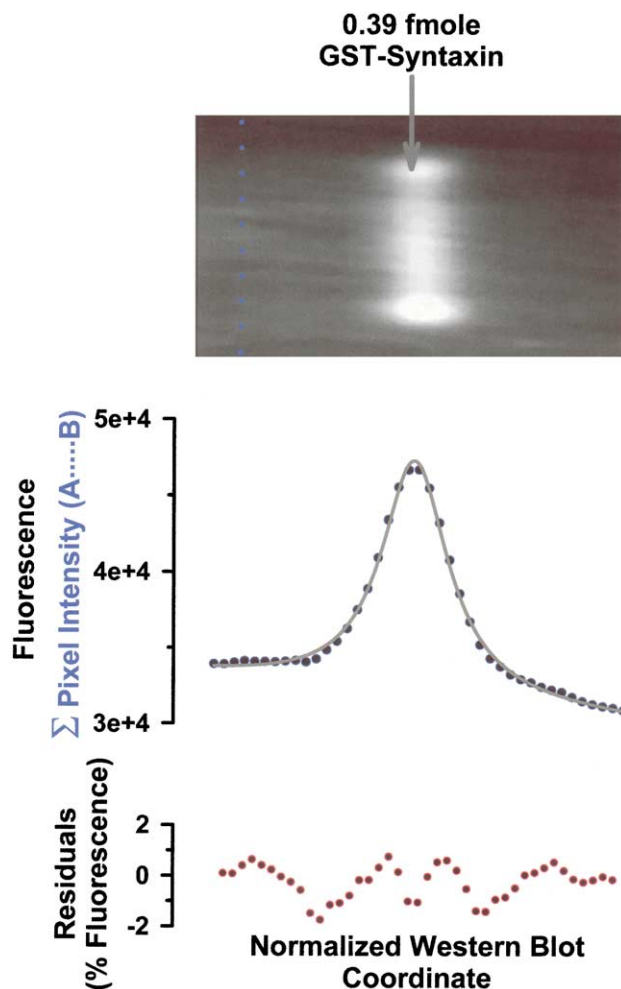
Fig. 2. Analysis of digitized ECF Western blot. The digitized ECF signal (pixel intensity) associated with 0.39 fmol of GST–syntaxin (top) was summed (lane scan) and plotted against the normalized Western blot coordinate (middle). The resulting curve was fit using a 5-parameter model (fluorescence $= A/(1 + (X - B)^2/C^2) + D * X + E$), where A is the peak amplitude, B is the peak midpoint, $2 * C$ is the full width at half maximum, D is the linear slope, E is the linear intercept, and X is the normalized Western blot coordinate associated with the position of the protein band in the membrane. The area under the peak was calculated using the relationship integrated peak fluorescence $= \pi * A * C$. The difference between the fitted function and the data, residuals, is shown as a measure of the goodness of fit associated with this procedure (bottom).
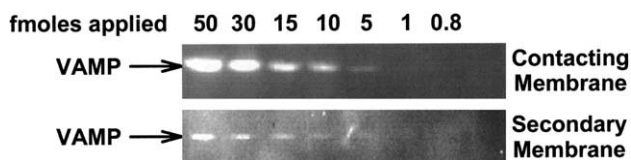

Fig. 3. Electrotransfer of VAMP through a 0.45-µm PVDF membrane. SDS–PAGE of the indicated amount of VAMP, followed by electrotransfer to a 0.45-µm PVDF membrane (contacting membrane) and a secondary 0.1-µm PVDF "backing" membrane resulted in the capture of VAMP on the second membrane after transfer through the first membrane. Loss of protein through a 0.45-µm PVDF membrane decreases calibration accuracy and sensitivity.

and methods) in order to obtain the most accurate and sensitive detection (Figs. 4 and 5) and checked for any further protein loss through the PVDF membranes. Under our conditions there was no detectable loss through 0.1-μm PVDF membranes. Preliminary data suggested that the limit of detection improved using the optimized 0.1-μm PVDF protocol instead of 0.45-μm PVDF membranes (64, 32, and 24% improvement for syntaxin, SNAP-25, and VAMP, respectively; $n = 1$); this improvement is in addition to the increase in accuracy expected from the elimination of detectable protein losses. In this regard, high sensitivity and optimal detection were also required to assess the amounts of SNAREs in samples (i) dominated by the high concentrations of other proteins (such as CV put directly into sample buffer) and (ii) having low protein concentrations, including aqueous phases from TX-114 extracts or organic precipitations.

Calibration detection limits and selectivity

The newly optimized immunoblotting protocol and associated analysis procedures yielded, on average, minimal detection limits of 4.4 ± 0.4 fmol VAMP ($n = 26$), 0.56 ± 0.04 fmol SNAP-25 ($n = 28$), and 0.05 ± 0.00 fmol syntaxin ($n = 32$) (mean ± SE). Typical calibration curves are shown in Fig. 4. Calibration curves were not altered by the presence of excess protein extracted from CV; sensitivity (calibration slope) was independent of other proteins present within the sample (Fig. 5). Absence of interference is absolute for SNAP-25 and VAMP because the standards migrate with the endogenous CV proteins, but there is no significant change in the sensitivity of the calibration; calibration was identical even after proteolytic removal of endogenous SNAP-25 and VAMP (Fig. 5A and B). GST–syntaxin, migrating at a higher molecular weight than native syntaxin, showed no interference when evaluated using two different amounts of CV material (Fig. 5C). Thus, the method is selective for the targeted proteins, preserving accuracy and sensitivity in the presence of high concentrations of other proteins.

Native CV SNARE complement

Hydrophobic proteins were extracted from fusion-competent CV immediately after isolation or following incubation in B-IM buffer (pH 6.7) for 1–4 h at 25 °C. No SNAREs were detected in aqueous phases of TX-114 extracts or $CHCl_3/CH_3OH$ precipitates. There was also no significant effect of the 1- to 4-h incubation times on the density of CV SNAREs (not shown). On average, isolated CV had 5450 ± 1260, 710 ± 140, and 330 ± 80 copies of VAMP ($n = 45$), SNAP-25 ($n = 43$), and syntaxin ($n = 43$), respectively (mean ± SE).

Discussion

We have developed and refined a highly sensitive quantitative immunoblotting analysis in order to determine the native SNARE density on fully functional secretory vesicles. Such routine high sensitivity resulted from systematic optimization of protein analyses including extraction and SDS–PAGE, immunoblotting, and chemifluorescence analysis (see Materials and methods). The ability to routinely and unambiguously identify and quantitatively assess specific proteins with (sub) femtomole accuracy and sensitivity provides a useful tool for rigorous analysis and understanding of proposed mechanisms involving these molecules and others.

SNARE membrane density

On average, each CV contains ~5450, 710, and 330 copies of VAMP, SNAP-25, and syntaxin, respectively. For an ~1 μm-diameter CV, these values correspond to average densities of ~1700, ~200, and ~100 copies/μm², respectively. For synaptic vesicles, native densities are estimated to be ~2800, ~500, and ~500 copies/μm², for VAMP, SNAP-25, and syntaxin, respectively, assuming a vesicle diameter of 45 nm [26]. The results indicate a marked similarity in SNARE densities on two different types of regulated secretory vesicles (CV and synaptic vesicles), suggesting that SNARE density may be a conserved feature of regulated vesicles, reflecting their function in the exocytotic pathway. However, substantially higher SNARE densities are required to achieve lipid mixing between liposomes containing reconstituted SNAREs: ~88,000, ~9400, and ~9400 copies/μm², for VAMP, SNAP-25, and syntaxin, respectively, assuming a vesicle diameter of 45 nm [6,27]. The requirement for a 50-fold increase in SNARE density compared to CV suggests that SNARE-mediated fusion of phospholipid vesicles may be another example of the ability of certain proteins to effect the fusion of artificial membrane systems [28–36]; in most instances this fusion occurs substantially faster than SNARE-mediated fusion and, like functional biological fusion, can be triggered by changes in $[Ca^{2+}]_{free}$ or pH.

Thus, Ca^{2+}-sensitive, fusion-competent, native vesicles function at their physiological optima with only a fraction of the SNARE density required in reconstituted systems. While SNARE reconstitution experiments indicate that *trans* SNARE complexes may contribute to membrane interactions that promote fusion in vivo, they are difficult to reconcile with an emerging body of work showing that for the fusion step of regulated exocytosis, additional proteins are essential downstream of the SNAREs, closer to the native triggered fusion event [2,3,9,10,16]. We are applying our quantitative immunoblotting method to further testing of the SNAREpin
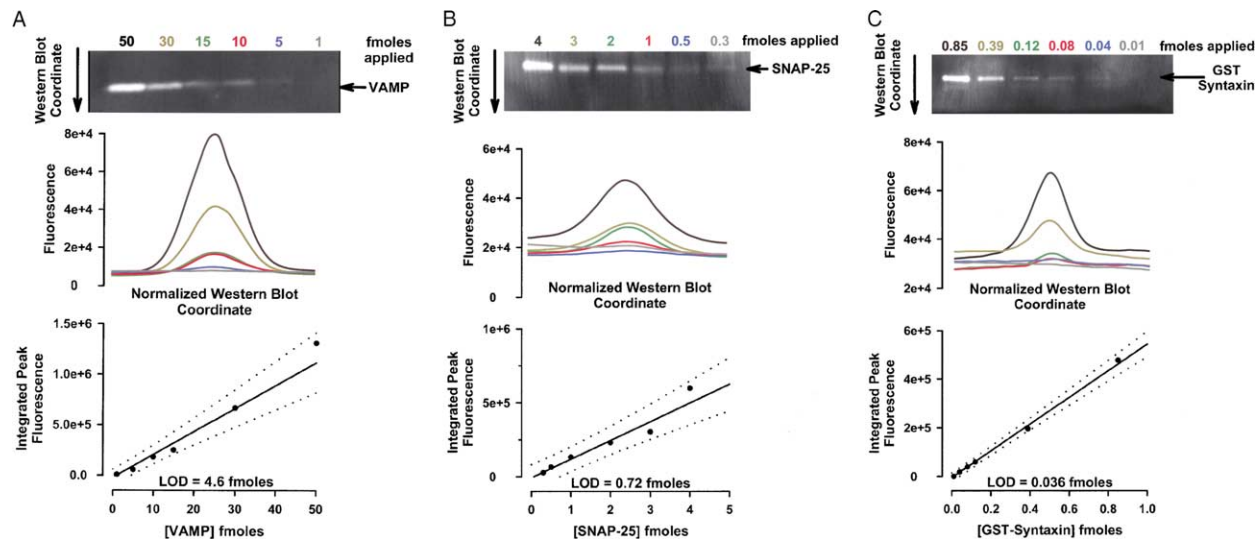
Fig. 4. Typical calibration curves. Typical examples of calibration curves associated with each of the three SNARE proteins. The top panels are the digitized ECF Western blots for (A) VAMP, (B) SNAP-25, and (C) syntaxin. The middle panels are the digitized lane scans that were fit using the Lorentzian + linear background function (see Fig. 2). Calibration curves (lower panels) were obtained using weighted linear regression of integrated peak fluorescence vs protein amount. The 95% prediction interval is indicated by the dotted lines. The limits of detection, defined as the amount of protein at a signal level three times the standard error of the fit, averaged over all calibration curves, are VAMP, 4.4 ± 0.4 fmol ($n = 26$); SNAP-25, $0.56 + 0.04$ fmol ($n = 28$); and syntaxin, 0.05 ± 0.00 fmol ($n = 32$).
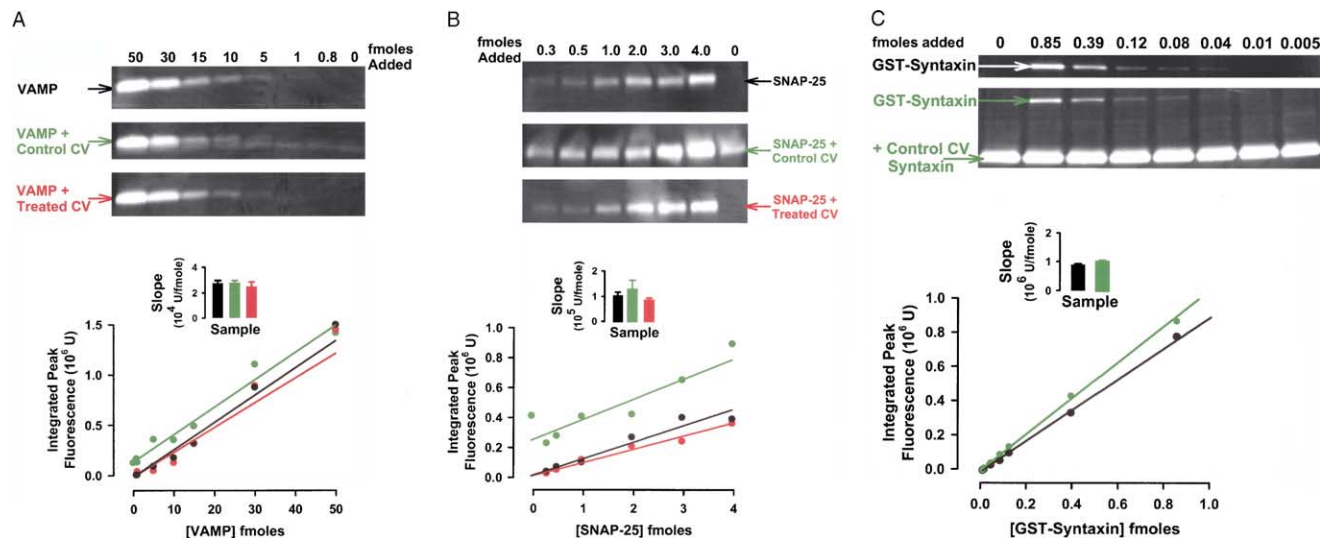

Fig. 5. Absence of interference. Addition of the indicated amounts of (A) VAMP, (B) SNAP-25, and (C) syntaxin to control CV, and VAMP, and SNAP-25 to CV enzymatically treated to reduce endogenous VAMP and SNAP-25 (top), resulted in calibration curves (bottom) with sensitivities (calibration slope, inset) invariant to the presence of endogenous proteins present in CV samples. There is no evidence of interference of other CV proteins with the immunodetection of SNAREs.

hypothesis. The ability to measure the amount and/or density of identified proteins is an unequivocal requirement for the quantitative testing of hypotheses. Quantitative Western blotting is an analytical tool that should prove more broadly useful in the analysis of other molecular mechanisms.

Acknowledgments

References

[1] H. Towbin, T. Staehelin, J. Gordon, Electrophoretic transfer of proteins from polyacrylamide gels to nitrocellulose sheets: procedure and some applications, Proc. Natl. Acad. Sci. USA 76 (1979) 4350–4354.

[2] W.N. Burnette, "Western Blotting": electrophoretic transfer of proteins from sodium dodecyl sulfate–polyacrylamide gels to unmodified nitrocellulose and radiographic detection with antibody and radioiodinated protein A, Anal. Biochem. 112 (1981) 195–203.

[3] E. Fernandez, J.J. Kopchick, Quantitative determination of growth hormone by immunoblotting, Anal. Biochem. 191 (1990) 268–271.

[4] J. Fradelizi, E. Friederich, M.C. Beckerle, R.M. Golsteyn, Quantitative measurement of proteins by western blotting with Cy5-coupled secondary antibodies, BioTechniques 26 (1999) 484–494.

[5] C. Rudolph, G. Adam, A. Simm, Determination of copy number of c-Myc protein per cell by quantitative Western blotting, Anal. Biochem. 269 (1999) 66–71.

[6] R.C. Lin, R.H. Scheller, Mechanisms of synaptic vesicle exocytosis, Annu. Rev. Cell Dev. Biol. 16 (2000) 19–49.

[7] J.R. Coorssen, P.S. Blank, M. Tahara, J. Zimmerberg, Biochemical and functional studies of cortical vesicle fusion: the SNARE complex and Ca^{2+} sensitivity, J. Cell Biol. 143 (1998) 1845–1857.

[8] J. Zimmerberg, P.S. Blank, I. Kolosova, M.-S. Cho, M. Tahara, J.R. Coorssen, A stage-specific preparation to study the Ca^{2+}-triggered fusion steps of exocytosis: rational and perspectives, Biochimie 82 (2000) 303–314.

[9] P.I. Hanson, R. Roth, H. Morisaki, R. Jahn, J.E. Heuser, Structure and conformational changes in NSF and its membrane receptor complexes visualized by quick-freeze/deep-etch electron microscopy, Cell 90 (1997) 523–535.

[10] Y.A. Chen, S.J. Scales, R.H. Scheller, Sequential SNARE assembly underlies priming and triggering of exocytosis, Neuron 30 (2001) 161–170.

[11] T. Weber, B.V. Zemelman, J.A. McNew, B. Westernmann, M. Gmachl, F. Parlati, T.H. Söllner, J.E. Rothman, SNAREpins: minimal machinery for membrane fusion, Cell 92 (1998) 759–772.

[12] R.B. Sutton, D. Fasshauer, R. Jahn, A.T. Brunger, Crystal structure of a SNARE complex involved in synaptic exocytosis at 2.4Å resolution, Nature 395 (1998) 347–353.

[13] S.Y. Hua, M.P. Charlton, Activity-dependent changes in partial VAMP complexes during neurotransmitter release, Nat. Neurosci. 2 (1999) 1078–1083.

[14] M. Tahara, J.R. Coorssen, K. Timmers, P.S. Blank, T. Whalley, R. Scheller, J. Zimmerberg, Calcium can disrupt the SNARE protein complex on sea urchin egg secretory vesicles without irreversibly blocking fusion, J. Biol. Chem. 273 (1998) 33667–33673.

[15] J.R. Coorssen, P.S. Blank, I. Kolosova, P. Backlund, J. Zimmerberg, Are SNARE proteins necessary and sufficient for membrane fusion?, Mol. Biol. Cell Suppl. S 10 (1999) 1269.

[16] J.R. Coorssen, P.S. Blank, F. Albertorio, L. Bezrukov, I. Kolosova, P. Backlund, J. Zimmerberg, Calcium-dependent homotypic fusion of exocytotic vesicles requires proteins with specific protease sensitivities but not SNARE proteins, 2002, submitted.

[17] S. Cannon-Carlson, J. Tang, Modification of the Laemmli sodium dodecyl sulfate–polyacrylamide gel electrophoresis procedure to eliminate artefacts on reducing and nonreducing gels, Anal. Biochem. 246 (1997) 146–148.

[18] P.G. Gillespie, S.K.H. Gillespie, Improved electrophoresis and transfer of picogram amounts of protein with hemoglobin, Anal. Biochem. 246 (1997) 239–245.

[19] A. Chrambach, The practice of quantitative gel electrophoresis, VCH Publishers, 1985.

[20] S.C. Gill, P.H. von Hippel, Calculation of protein extinction coefficients from amino acid sequence data, Anal. Biochem. 182 (1989) 319–326.

[21] P. Foran, G. Lawrence, J.O. Dolly, Blockade by botulinum neurotoxin B of catecholamine release from adrenochromaffin cells correlates with its cleavage of synaptobrevin and a homologue present on granules, Biochemistry 34 (1995) 5494–5503.

[22] G.H. Weiss, H. Sokoloff, S.F. Zakharov, A. Chrambach, Interpretation of electrophoretic band shapes by a partition chromatographic model, Electrophoresis 17 (1996) 1325–1332.

[23] V.B. Di Marco, G.G. Bombi, Mathematical functions for the representation of chromatographic peaks, J. Chromatogr. A 931 (2001) 1–30.

[24] W. Lin, H. Kasamatsu, On the transfer of polypeptides from gels to nitrocellulose membranes, Anal. Biochem. 128 (1983) 302–311.

[25] M.W. Bolt, P.A. Mahoney, High-efficiency blotting of proteins of diverse sizes following sodium dodecyl sulfate–polyacrylamide gel electrophoresis, Anal. Biochem. 247 (1997) 185–192.

[26] C. Walch-Solimena, J. Blasi, L. Edelmann, E.R. Chapman, G. Fischer von Mollard, R. Jahn, The t-SNAREs syntaxin 1 and SNAP-25 are present on organelles that participate in synaptic vesicle recycling, J. Cell Biol. 128 (1995) 637–645.

[27] J.A. McNew, F. Parlati, R. Fukuda, R.J. Johnston, K. Paz, F. Paumet, T.H. Söllner, J.E. Rothman, Compartment specificity of cellular membrane fusion encoded in SNARE proteins, Nature 407 (2000) 153–159.

[28] C.E. Creutz, cis-Unsaturated fatty acids induce the fusion of chromaffin granules aggregated by synexin, J. Cell Biol. 91 (1981) 247–256.

[29] S. Schenkman, P.S. De Araujo, A. Sesso, F.H. Quina, H. Chaimovich, A kinetic and structural study of two-step aggregation and fusion of neutral phospholipid vesicles promoted by serum albumin at low pH, Chem. Phys. Lipids 28 (1981) 165–180.

[30] R. Blumenthal, M. Henkart, C.J. Steer, Clathrin-induced pH-dependent fusion of phosphatidylcholine vesicles, J. Biol. Chem. 258 (1983) 3409–3415.

[31] R. Sundler, J. Wijkander, Protein-mediated intermembrane contact specifically enhances Ca^{2+}-induced fusion of phosphatidate-containing membranes, Biochim. Biophys. Acta 730 (1983) 391–394.

[32] T.M. Young, J.D. Young, Protein-mediated intermembrane contact facilitates fusion of lipid vesicles with planar bilayers, Biochim. Biophys. Acta 775 (1984) 441–445.

[33] G. Fujii, M.E. Selsted, D. Eisenberg, Defensins promote fusion and lysis of negatively charged membranes, Protein Sci. 2 (1993) 1301–1312.

[34] M. Otter-Nilsson, R. Hendriks, E.I. Pecheur-Huet, D. Hoekstra, T. Nilsson, Cytosolic ATPases, p97, and NSF, are sufficient to mediate rapid membrane fusion, EMBO J. 18 (1999) 2074–2083.

[35] B. Brügger, W. Nickel, T. Weber, F. Parlati, J.A. McNew, J.E. Rothman, T. Söllner, Putative fusogenic activity of NSF is restricted to a lipid mixture whose coalescence is also triggered by other factors, EMBO J. 19 (2000) 1272–1278.

[36] A. Agirre, S. Nir, J.L. Nieva, J. Dijkstra, Induction of aggregation and fusion of cholesterol-containing membrane vesicles by an anti-cholesterol monoclonal antibody, J. Lipid Res. 41 (2000) 621–628.